# Structural properties and constructability of composite members

# Structural Properties and Constructability
# of Composite Members

## Caractéristiques structurales et aptitude à la construction de membrures mixtes

## Tragwerkseigenschaften und Betonierungsfähigkeit von Verbundbauteilen

**T. SHIOYA**
Senior Res. Engineer
Shimizu Corporation
Tokyo, Japan

Toshiyuki Shioya, born in 1950, received his degree of Dr. of Engineering from the University of Tokyo. His main fields of research are shear problems of reinforced concrete and composite structures.

**H. OOUCHIDA**
Manager
Shimizu Corporation
Tokyo, Japan

Hiroki Oouchida, born in 1947, received his B.Sc. and M.Sc. degrees in Civil Engineering from Kyushu University. He has been working on design of offshore structures.

**T. HASEGAWA**
Research Engineer
Shimizu Corporation
Tokyo, Japan

Toshiaki Hasegawa, born in 1958, received his B.Sc. and M.Sc. degrees in Civil Engineering from Waseda University. His main research interest is fracture mechanics of concrete.

**F. OHNO**
Civil Engineer
Shimizu Coporation
Tokyo, Japan

Fumiyoshi Ohno, born in 1957, received a degree in Civil Engineering from the Science University of Tokyo and another in Computer and Information Science from the Univ. of Oregon, USA. He is working on offshore engineering.

## SUMMARY
Presented are the results of structural and constructability tests of a composite steel/concrete structure using a steel sandwiched concrete system for the purpose of establishing the design and construction methods. It was confirmed by flexure and shear tests that the composite members have high ductility when compared with reinforced concrete members. Sufficient infilling and effectiveness of a continuous concreting system were confirmed in mock-up tests.

## RÉSUMÉ
Cet article décrit les résultats d'essais structuraux et d'aptitude à la construction d'une construction mixte acier/béton qui utilise un système de béton armé type sandwich avec le but d'établir des méthodes de conception et de construction. On a pu confirmer à l'aide d'essais de flexion et de cisaillement que les membrures mixtes possèdent une ductilité élevée, comparées aux membrures en béton armé. En outre, des essais de maquette ont confirmé un remplissage et une efficacité adéquats d'un système de bétonnage continu.

## ZUSAMMENFASSUNG
Die Ergebnisse von Tragfähigkeits- und Betonierungsfähigkeitsprüfungen an einem Verbundtragwerk werden vorgestellt. Diese Prüfungen wurden durchgeführt, damit die Entwurfs- und Betonierungsmethoden entwickelt werden können. Bei den Biegungs- und Schubprüfungen zeigte sich, daß die zusammengesetzten Bauteile im Vergleich zu normalen Stahlbetonbauteilen eine höhere Duktilität haben. Durch Betonierungsfähigkeitsprüfungen wurden Füllgrad und die Wirksamkeit des Systems bestätigt.

## 1. INTRODUCTION

Arctic offshore structures are subjected to severe ice loads. A composite member in which concrete is injected into a steel encasement is remarkably well suited for use in such conditions because of its excellent ductility and high strength[1][2]. It can facilitate the potential to improve the constructability of the structure, resulting in the reduction of construction costs and time needed. However, practical methods for construction and design of such a composite member have not been fully established yet. Therefore extensive research work was carried out to verify the strength characteristics and to develop an applicable construction procedure.

## 2. FLEXURE TEST

### 2.1 Outline of test

To investigate the buckling behavior of compression plates under flexural loading, 13 flexural tests were performed. Dimensions and basic configurations are shown in Fig. 1. The parameters in the flexure tests are as follows:

(A) Height of stiffeners : $h_f$
(B) Spacing of stiffeners : $l_f$
(C) Direction of stiffeners ;

    A-type : stiffeners were set longitudinally
    B-type : stiffeners were set transversely

In addition, a reinforced concrete model, having the same steel ratio as the composite test model, was tested. The target compressive strength of the concrete was approximately 45MPa. Mix proportions are shown in Table 2. Steel properties are shown in Table 1. The tests were carried out using a 4-point bending configuration as illustrated in Fig. 1.
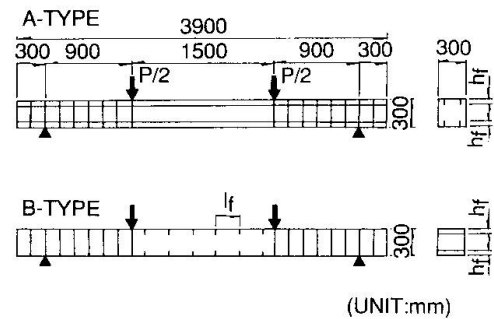


Fig. 1 Flexure test models and loading configurations

### 2.2 Result of flexure tests

**(1) Load deflection relation curves**
The deflections measured at midspan under flexural loading are shown in Fig. 2. For the composite models, unless elastic buckling of the compression plate took place, failure occurred due to plastic buckling of the compression plate after 8 to 10 times the deflection at yield. For the reinforced concrete model, compared with the composite models, it failed with the crushing of the concrete at smaller deflection. In short, the composite members had a higher ductile capacity under flexural loading.
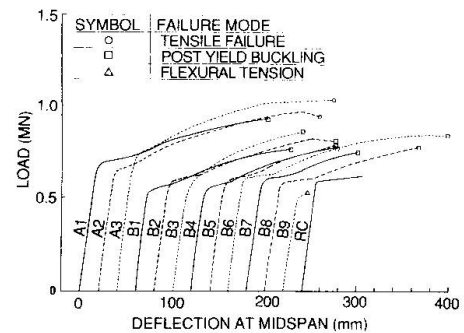


Fig. 2 Load - deflection curves

**(2) Flexural failure strength**
Figure 3 shows the ratios between the experimental yield moment and the calculated value based on conventional RC (Reinforced Concrete) beam theory. It turns out that the experimental yield moment agreed well with that calculated by the RC theory. It was observed, up to the yield load, that at the section in constant moment span the "plane sections before bending remain plane after bending" assumption can be made for the composite members. The composite member showed a higher



Fig. 3 Experimental/calculated yield moment

## Table 1 Varieties of models and principal test results

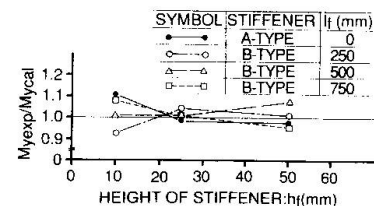| Test | Test model | Length L (mm) | Loading span l (mm) | Effective depth d (mm) | Breadth b (mm) | Mix | Comp. strength f'c (MPa) | Splitting tensile strength f't (MPa) | Thickness t (mm) | Yield strength $f_{sy}$ (MPa) | Tensile strength $f_{st}$ (MPa) | Main steel ratio p (%) | Type | Height $h_f$ (mm) | Spacing $l_f$ (mm) | Yield load $P_y$ (MN) | Buckling load $P_b$ (MN) | Maximum load $P_{max}$ (MN) | Maximum moment $M_{max}$ (MN·m) | Maximum shear strength (MPa) | Failure mode |
|---|---|---|---|---|---|---|---|---|---|---|---|---|---|---|---|---|---|---|---|---|---|
| Flexure | A1 | 3900 | 3300 | 296 | 300 | M1 | 41.5 | 2.78 | 9 | 324 | 520 | 3.05 | A | 10 | – | 0.667 | 0.937 | 0.937 | 0.422 | – | Post yield buckling |
| | A2 | 3900 | 3300 | 296 | 300 | M1 | 43.3 | 2.91 | 9 | 324 | 520 | 3.05 | A | 25 | – | 0.647 | ~ | 0.981 | 0.441 | – | Discontinuance due to support-slip |
| | A3 | 3900 | 3300 | 296 | 300 | M1 | 43.7 | 2.93 | 9 | 324 | 520 | 3.05 | A | 50 | – | 0.745 | ~ | 1.06 | 0.477 | – | |
| | B1 | 3900 | 3300 | 296 | 300 | M1 | 44.0 | 2.96 | 9 | 324 | 520 | 3.05 | B | 10 | 250 | 0.549 | 0.780 | 0.780 | 0.351 | – | Post yield buckling |
| | B2 | 3900 | 3300 | 296 | 300 | M1 | 45.5 | 3.07 | 9 | 324 | 520 | 3.05 | B | 25 | 250 | 0.588 | 0.814 | 0.843 | 0.380 | – | Post yield buckling |
| | B3 | 3900 | 3300 | 296 | 300 | M1 | 46.1 | 3.11 | 9 | 324 | 520 | 3.05 | B | 50 | 250 | 0.569 | 0.863 | 0.873 | 0.393 | – | Post yield buckling |
| | B4 | 3900 | 3300 | 296 | 300 | M1 | 46.3 | 3.13 | 9 | 324 | 520 | 3.05 | B | 10 | 500 | 0.569 | 0.789 | 0.789 | 0.355 | – | Post yield buckling |
| | B5 | 3900 | 3300 | 296 | 300 | M1 | 46.8 | 3.18 | 9 | 324 | 520 | 3.05 | B | 25 | 500 | 0.588 | 0.794 | 0.804 | 0.362 | – | Post yield buckling |
| | B6 | 3900 | 3300 | 296 | 300 | M1 | 46.9 | 3.20 | 9 | 324 | 520 | 3.05 | B | 50 | 500 | 0.608 | 0.873 | 0.873 | 0.393 | – | Post yield buckling |
| | B7 | 3900 | 3300 | 296 | 300 | M1 | 47.3 | 3.23 | 9 | 324 | 520 | 3.05 | B | 10 | 750 | 0.608 | 0.760 | 0.760 | 0.342 | – | Post yield buckling |
| | B8 | 3900 | 3300 | 296 | 300 | M1 | 47.4 | 3.25 | 9 | 324 | 520 | 3.05 | B | 25 | 750 | 0.588 | 0.809 | 0.809 | 0.364 | – | Post yield buckling |
| | B9 | 3900 | 3300 | 296 | 300 | M1 | 47.9 | 3.30 | 9 | 324 | 520 | 3.05 | B | 50 | 750 | 0.539 | 0.294 | 0.539 | 0.243 | – | Flexural tension |
| | RC | 3950 | 3300 | 300 | 300 | M1 | 46.3 | 3.48 | #6x10* | 343 | 520 | 3.19 | – | – | – | 0.569 | – | 0.642 | 0.289 | – | Flexural tension |
| Shear | CBR | 4000 | 1800 | 618 | 590 | M2 | 59.4 | 2.59 | 12 | 304 | 441 | 1.94 | RIB | 550 | 350 | – | – | 2.17 | – | 5.95 | Shear compression |
| | CBF | 4000 | 1800 | 618 | 590 | M2 | 56.8 | 3.11 | 12 | 304 | 441 | 1.94 | FB | 100 | 200 | – | – | 3.23 | – | 8.86 | Shear compression |
| | CSR | 4000 | 1800 | 618 | 1190 | M2 | 59.4 | 3.05 | 12 | 304 | 441 | 1.94 | RIB | 550 | 350 | – | – | 5.80 | – | 7.88 | Shear compression |
| | CSF | 4000 | 1800 | 618 | 1190 | M2 | 56.8 | 3.00 | 12 | 304 | 441 | 1.94 | FB | 100 | 200 | – | – | 6.67 | – | 9.11 | Shear compression |
| | RCB | 4000 | 1800 | 600 | 600 | M2 | 55.3 | 2.74 | #10x9* | 343 | 549 | 1.99 | – | – | – | – | – | 2.73 | – | 7.58 | Shear compression |
| | CBFS | 2012 | 900 | 309 | 300 | M2 | 56.7 | 3.72 | 6 | 358 | 409 | 1.94 | FB | 50 | 100 | – | – | 1.20 | – | 12.8 | Shear compression |
| | A | 3000 | 2400 | 296 | 300 | M1 | 40.3 | 2.70 | 9 | 324 | 520 | 3.05 | A | 50 | – | – | – | 0.361 | – | 4.04 | Tied-arch |
| | B | 3000 | 2400 | 296 | 300 | M1 | 40.7 | 2.73 | 9 | 324 | 520 | 3.05 | B | 50 | 300 | – | – | 0.108 | – | 1.20 | Diagonal tension |

(Note) *:Deformed reinforcing bars

## Table 2 Mix proportions of concrete

| Mix | Target comp. strength f'c (MPa) | Maximum size of coarse aggregate $G_{max}$ (mm) | Range of slump (cm) | Range of air content (%) | Water-cement ratio W/C (%) | Sand-agg. ratio s/a (%) | Unit content (kg/m³) | | | | |
|---|---|---|---|---|---|---|---|---|---|---|---|
| | | | | | | | Water W | Cement C | Silica fume SF | Sand S | Gravel G |
| M1 | 45 | 25* | 24±2 | 5±2 | 35 | 39 | 157 | 450 | – | 646 | 1042 |
| M2 | 50 | 15** | >25 | 7±2 | 29 | 38 | 146 | 502 | 50 | 589 | 598 |

(Note) * :Normal weight coarse aggregate
    **:Light weight coarse aggregate

increase of strength from yield strength to ultimate strength in comparison with the corresponding reinforced concrete member. For the estimation of ultimate strength, we may take into account the effect of strain hardening state of steel, and the effect of enhanced concrete strength due to multiaxial confinement.

## 3. SHEAR TEST

### 3.1 Outline of test

To evaluate shear strength of composite beams and slabs with different inner configurations, 7 shear tests were performed. The dimensions and basic configurations are shown in Fig. 4. Four types of stiffener configurations were considered, they were as follows:

(A) FB-type: Lattice shaped flat bars were set.

(B) RIB-type: L-shaped stiffeners were set transversely.

(C) A-type: Stiffeners were set longitudinally.

(D) B-type: Stiffeners were set transversely.

Furthermore, a RCB (Reinforced Concrete Beam) model, having the same steel ratio as the RIB type models, was tested to compare the shear strength. The target compressive strength of concrete was 45 to 50 MPa. Mix proportions are shown in Table 2. Steel properties are shown in Table 1. The tests were carried out using simply supported configurations with two or four point concentrated loadings as illustrated in Fig. 4.

### 3.2 Result of shear test

(1) Shear stress deflection relation of FB, RIB, RCB-type models

The deflections of FB, RIB, RCB-type models measured at mid-span under shear loading are shown in Fig. 5. It was confirmed that the composite members are superior in resisting earthquake loads by the fact that the energy absorbing capacity for the CBR model is 5 times greater than for the RCB model, and for other models is more than 20 times greater than that for the RCB model.

(2) Ultimate shear strength of FB, RIB, RCB-type models

Figure 6 shows ratios between the experimental shear strengths and values calculated by the JSCE (Japan Society of Civil Engineers) equation[3] for deep beams and by the ACI equation[4]. The calculation by the JSCE equation showed a good agreement with the experimental results, and calculation by the ACI equation gave relatively conservative results. The JSCE equation is expressed as;

$$\tau_D = 3.0 \ (d/100)^{-1/4} \ (100 p_w)^{1/3} \ f'_c{}^{1/2}/[1+(a_v/d)^2], \quad (1)$$
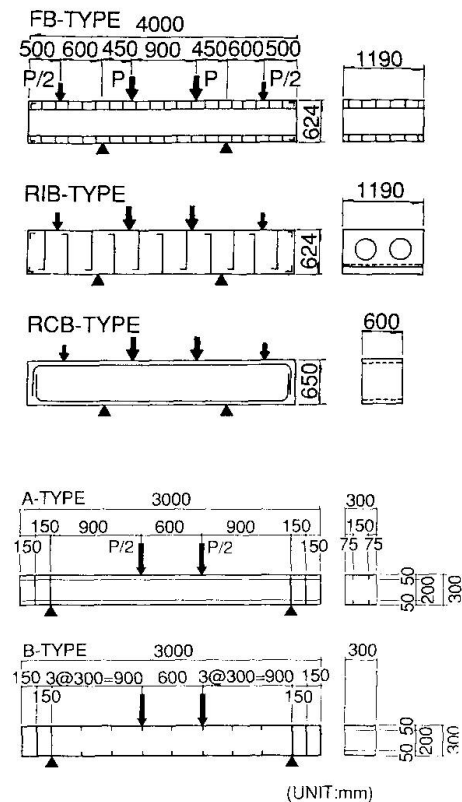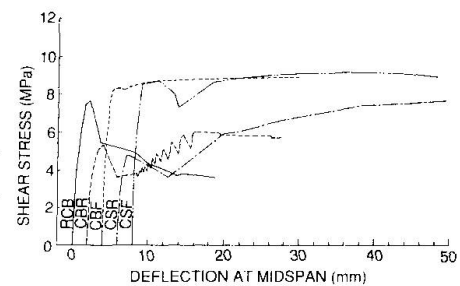


Fig. 4 Shear test models and loading configurations
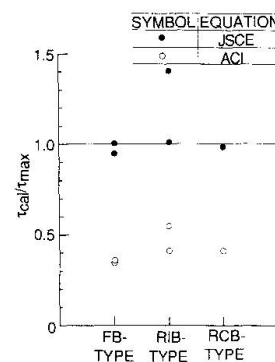


Fig. 5 Shear stress - deflection curves



Fig. 6 Experimental/calculated shear strength

where, $\tau_D$: shear strength of deep beam (kgf/cm²), d: effective depth (cm), $p_w$: longitudinal tension reinforcement ratio, $a_v$:shear span length less half of the support plate width (cm), f'c: compressive strength of concrete (kgf/cm²)

(3) The effect of stiffener direction on shear strength
Figure 7 shows the ratio between experimental shear strengths of A-type and B-type beams and calculations by the JSCE equation for slender beams. Stiffeners were set longitudinally in the A-type beam and transversely in the B-type beam. The B-type beam failed in shear. Although the A-type beam failed in flexure, the maximum shear stress of the A-type beam was three times larger than that of the B-type beam. It was observed that transversal stiffeners became the trigger of diagonal tension cracks. Therefore, there are some cases where beams with no transversal stiffener have larger shear strength. The JSCE equation is expressed as;

$$\tau_c=0.94f'c^{1/3} \beta_p \beta_d [0.75+1.4/(a/d)], \qquad (2)$$
$$p_w=100 A_s/(b_w d), \beta_p=p_w^{1/3} <1.5,$$
$$\beta_d=d^{-1/4} <1.5, d[m]$$

where, $\tau_c$: ultimate shear strength (kgf/cm²), f'c: compressive strength of concrete (kgf/cm²), a: shear span, d: effective depth, $b_w$: breadth of web, $A_s$: cross-sectional area of tension reinforcing bars.

(4) Size effect on shear strength of composite beam.
The deflections of CBF and CBFS models measured at midspan under shear loading are shown in Fig. 8. The CBFS model is a half scale of the CBF model. The nominal shear strength decreased as the beam size increased. Therefore, when designing large composite members, it is necessary to consider the size effect on shear strength. Figure 9 shows the ratios of the values calculated by JSCE equation for deep beam to the experimental shear strength. The JSCE equation showed a good agreement with the experimental shear strengths.

4. CONSTRUCTABILITY TEST

4.1 Outline of test

To aid in the development of a practical construction procedure, 18 injection tests were carried out. Details of the injection tests are described in Ref. 1. After the injection tests, in order to confirm the applicability of the concrete placing system achieved through the injection tests the large constructability test was performed. The test models are shown in Fig. 10, acrylic plates were used
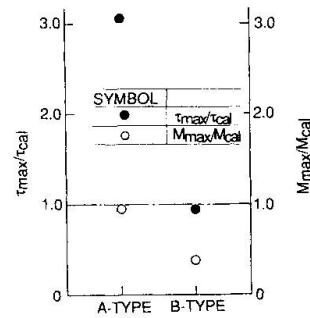


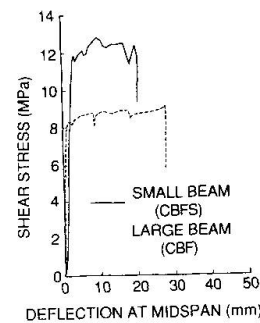Fig. 7 Calculated/experimental shear strength


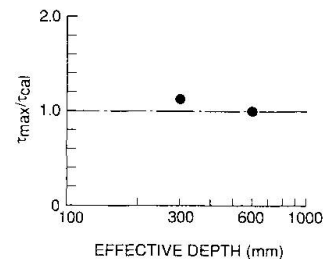
Fig. 8 Shear stress - deflection curves



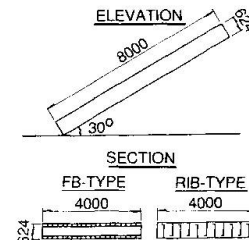Fig. 9 Experimental/calculated shear strength



Fig. 10 Large constructability test models

on the surface of the models to allow visual inspection. The concrete injecting system is shown in Fig. 11, the system employs valve controlled multiple outlets using flexible tremie pipes which are continuously inserted and elevated. The pipes are equipped with vibrators for consolidation.

### 4.2 Result of constructability test

The results are summarized as follows;
(1) Perfect injection was observed.
(2) Although the maximum temperature rise of concrete was 68°C, no cracks on the concrete surface were observed.

Fig. 11 Concrete injecting system

(3) The injection equipment operated well. The result confirmed that it can be applicable in the actual construction. From the test, the placing rate is estimated to be approximately 40m³/hr.
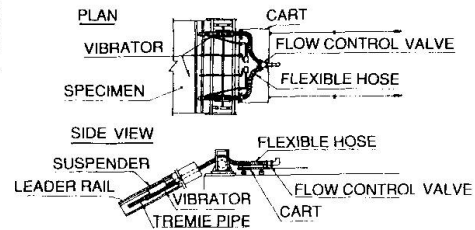
## 5. CONCLUSION

(1) Flexural tests confirmed that the yield moment of composite members can be calculated using the conventional theory for reinforced concrete. The composite beams showed a high ductility. Failure occurred when deflection reached 10 times the yield deflection. The failure modes of the composite beams were compression plate buckling and concrete crushing. As for the reinforced concrete beam, failure occurred, prior to such large deflection, due to crushing of concrete in the compression region.

(2) The shear strength of the composite members is almost the same as that of reinforced concrete members as long as an appropriate inner stiffener configuration is employed. It is observed that calculation by the JSCE (JSCE: Japan Society of Civil Engineers) equation agreed well with the experimental results, and the calculation by the ACI equation showed relatively conservative results. In addition, the composite member showed extremely large energy absorption capacity, 20 times larger than that of a reinforced concrete beam. However, inner stiffeners induced the shear failure of the beam. Without inner transverse stiffeners, shear strength of the beam becomes larger.

(3) The shear strength of the composite beam decreased as the depth of the beam increases (size effect on shear strength). Therefore, when designing composite beams, it is necessary to consider the size effect on shear strength.

(4) A concrete placing system that enables continuous placement of highly plastic and segregation-free concrete into intricate steel encasements was developed. Sufficient infilling of concrete and the effectiveness of the system were confirmed in mock-up tests.

## REFERENCES

1. SHIOYA T., MATSUMOTO G. et al., Development of Composite Members for Arctic Offshore Structures. Proc. of POLARTECH '86, Vol.2, Oct. 1986, pp.660-677.
2. OHNO F., SHIOYA T. et al., Experimental Studies on Composite Members for Arctic Offshore Structures. POAC '87 (to appear).
3. JSCE, Standard Specification for Design and Construction of Concrete Structures- 1986, part 1 (Design). 1986.
4. ACI, Building Code for Reinforced Concrete(318-83). 1983.